

Mesoscale Gravity Waves in Moist Baroclinic Jet-Front Systems

Junhong Wei

Current Position: Postdoc in Goethe University of Frankfurt

The main part of this talk comes from my dissertation at Penn State (Advisor: Fuqing Zhang; Sponsored by NSF), as well as the visit in NCAR (Hosted and Advised by Jadwiga H. Richter).

With travel support from WCRP

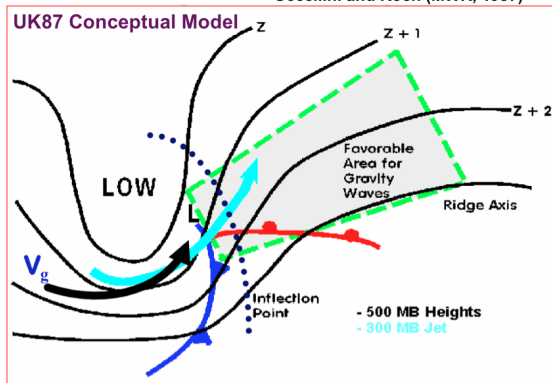
Section 1

- 1 Introduction
- 2 Idealized Moist Jet/Front Waves
- 3 Spectral Characteristics
- 4 Conclusion

UK87 Conceptual Model

Jet/Front Gravity Waves: Synoptic Environment

Uccellini and Koch (MWR, 1987)



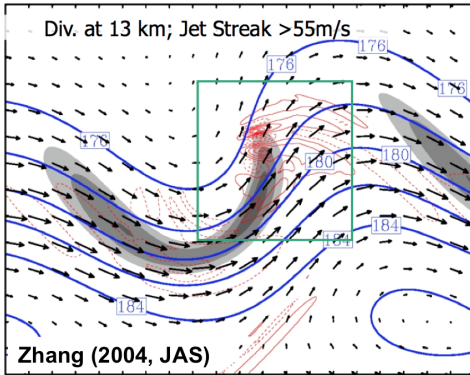
Common

Wave Characteristics

- $\lambda_H \sim 50-500 \text{ km}$
- $\lambda_z \sim 1-4 \text{ km}$
- $C_p \sim 15-35 \text{ m/s}$

- Preferred region: vicinity of upper jet; cold side of surface front
- Leading hypothesis of wave generation: geostrophic adjustment

Dry Idealized Simulations



Multiply nested mesoscale numerical simulations (MM5) with horizontal resolution up to 3.3km

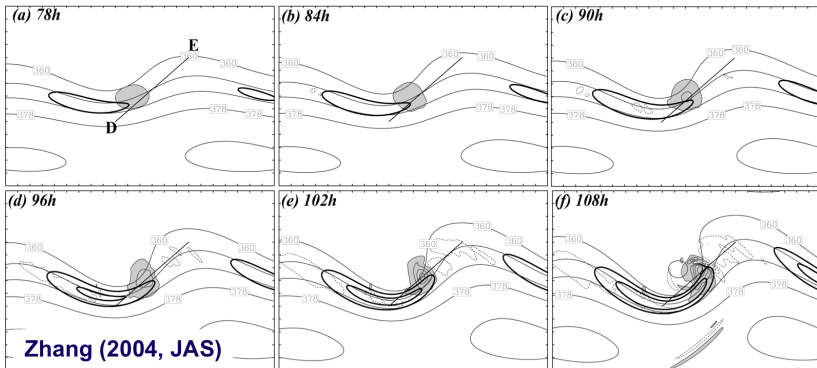
- Wave characteristics (Zhang Wave):
 $\lambda_H \sim 150\text{km}$ (mesoscale); $\lambda_z \sim 2.5\text{km}$; $\Omega \sim 4f$
- Hypothesized generation mechanism:
spontaneous balance adjustment

Spontaneous Balance Adjustment

Flow imbalance diagnosed with nonlinear balance equation

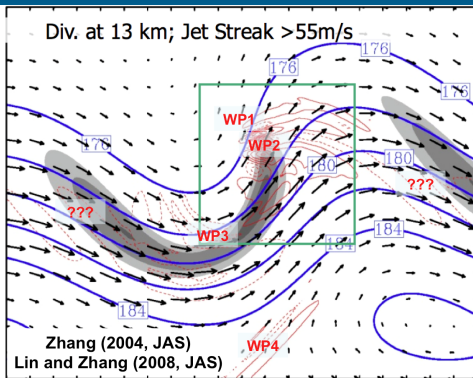
(Gray: pressure, every 5hPa; Bold: winds > 55m/s;
Thin: ΔNBE , positive, solid & shaded, negative, dashed)

$$\Delta NBE = 2J(u, v) + f\zeta - \nabla^2\Phi$$



- Increasing imbalance maximizes at jet exit region, and gravity waves are continuously initiated downstream of maximum imbalance
- Hypothesized generation mechanism: spontaneous balance adjustment (a generalization of the geostrophic adjustment)

Tracking Gravity Waves in Dry Simulations



- Lin and Zhang (2008, JAS): A 2D Fourier decomposition is employed to identify four simulated wave packets: WP1-WP4.
- Plougonven and Snyder (2007, JAS): The fifth wave packet between the ridge and the trough

	λ_H	λ_z	Ω	Potential Source
WP1	150km	2.6km	3.7f	upper jet or surface front
WP2	350km	2.9km	2.0f	upper jet
WP3	140km	5.0km	7.0f	surface front
WP4	NA	NA	NA	surface front

Motivation

Why taking moisture and heating into consideration?

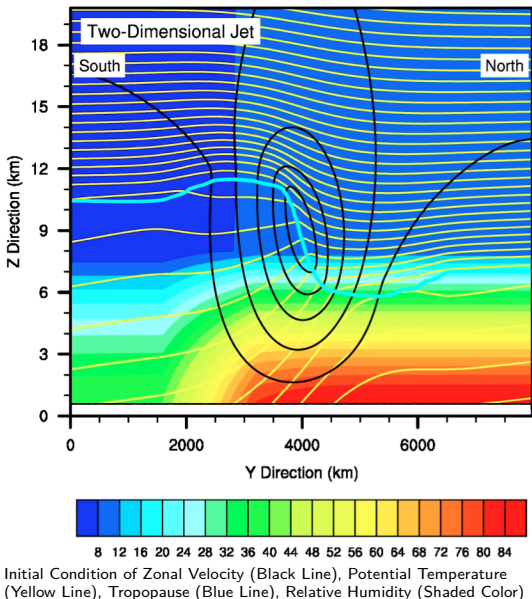
- Moist convection is closely linked with mesoscale gravity waves in the jet-front baroclinic waves. Moist convection itself is an important source of gravity waves, and it is an active and significant contributor to the development of the baroclinic waves and flow imbalance.
- Parameterizations of nonographic gravity waves (potential sources: convection, jet and front) remains a great challenge, and it is important to explore the gravity wave spectral characteristics among moist baroclinic jet-front systems with varying degree of convective instability.

Please also refer to Plougonven and Zhang (2014, Rev. Geophys.) for the current knowledge and understanding on gravity waves near jets and fronts from observations, theory, and modeling.

Section 2

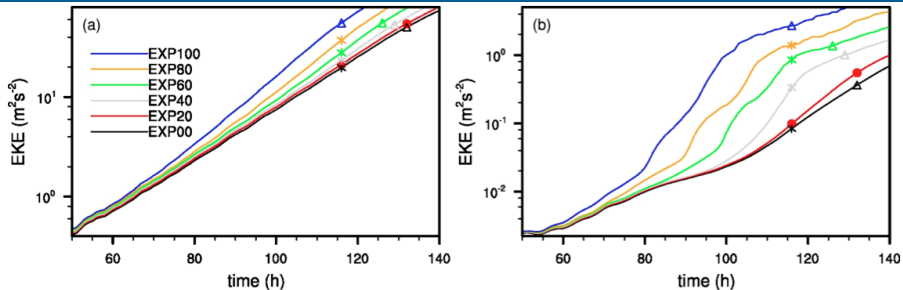
- 1 Introduction
- 2 Idealized Moist Jet/Front Waves
- 3 Spectral Characteristics
- 4 Conclusion

Model Setup



- WRF-ARW version 3.4
- $\Delta x = \Delta y = 10 \text{ km}$;
 $\Delta z \approx 300 \text{ m}$
- Zero RH in EXP00.
- The initial RH in EXP100 (shaded color) refers to the corrigendum (Tan et al. 2008) for Tan et al. (2004).
- EXP80 (EXP60; EXP40; EXP20) reduces its initial RH to 80% (60%; 40%; 20%) of that in EXP100.
- The six runs of EXP100-EXP00 have the same initial jet.

Eddy Kinetic Energy Growth



Time series (h) of eddy kinetic energy (m^2s^{-2}) for (a) EKE-BW (baroclinic wave component), (b) EKE-GW (gravity wave component) during 50-140 h.

Same Initial
Baroclinic Jet
+
Higher initial
Moisture Content



➤ Faster growth of baroclinic wave in terms of eddy kinetic energy (EKE-BW)

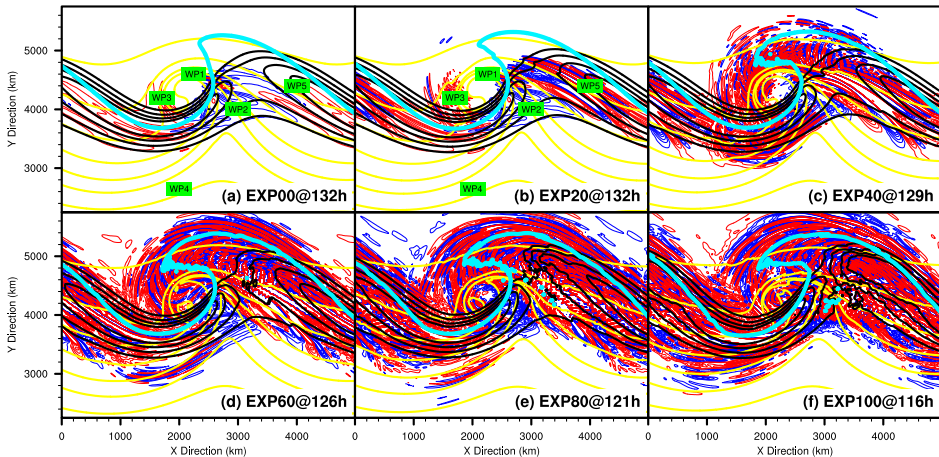


➤ Faster growth of eddy kinetic energy for gravity waves (EKE-GW)



➤ Greater EKE-GW when EKE-BW at similar amplitude of $\sim 52.5 m^2s^{-2}$

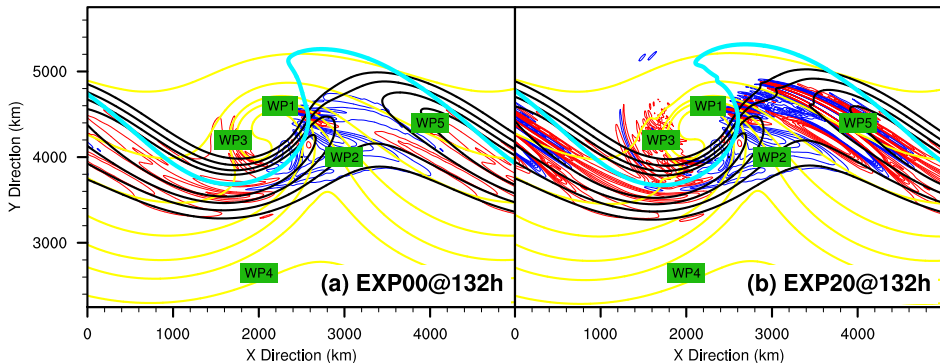
Simulations with Varying Initial Moisture



Simulated 1-km temperature (yellow lines), 8-km horizontal wind (black lines), 12-km horizontal divergence (blue/red lines)

- Simulations of moist baroclinic life cycles suggest a much more energetic gravity wave field than in dry simulations.

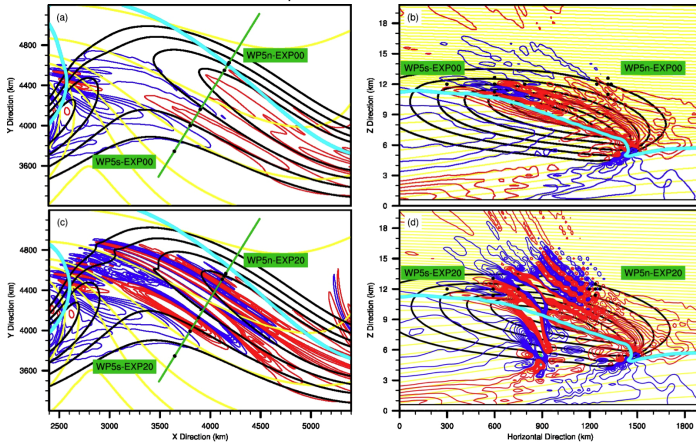
Weak Convective instability



- EXP00: Dry Localized Identifiable Gravity Wave Modes Generated By Dry Source
- EXP20: Dry Gravity Wave Modes Continue to Dominate; Similar Wave Characteristics With those in EXP00; The Amplitude of WP5 Is Enhanced; Modification in WP3.

The Fifth Wave Packets

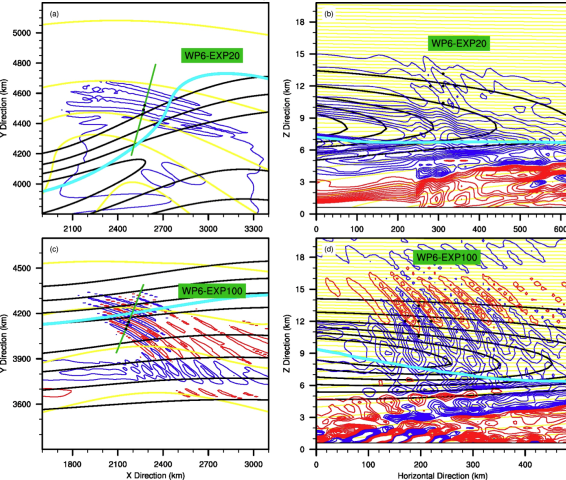
Examples of WP5s and WP5n



	λ_H	λ_z	Ω		λ_H	λ_z	Ω
WP5n-EXP00	90km	1.6km	3.9f	WP5s-EXP00	490km	1.4km	1.2f
WP5n-EXP20	68km	1.1km	3.6f	WP5s-EXP20	450km	1.7km	1.3f

Convectively Generated Wave Packets

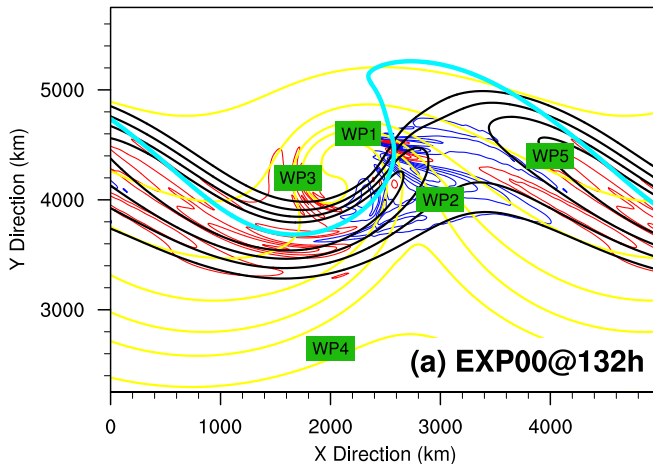
Examples of WP6



	λ_H	λ_z	Ω
WP6-EXP20	62km	2.8km	9.2f
WP6-EXP100	50km	2.9km	12.0f

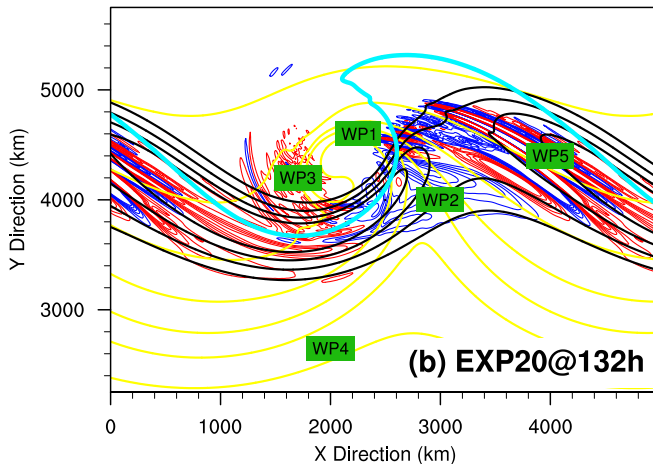
- A new wave packet

Gravity Wave Field in Dry Run



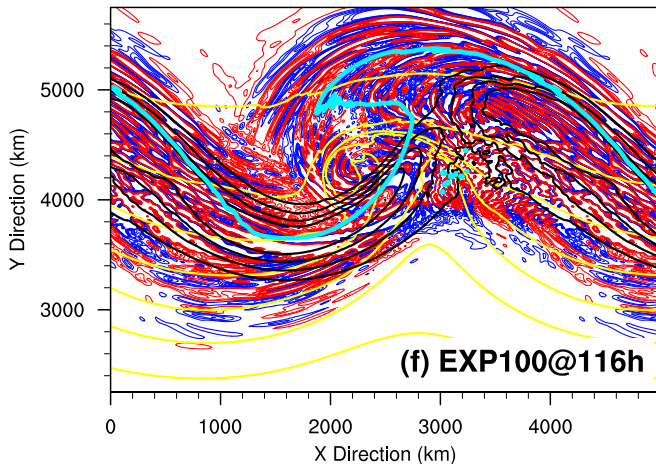
- Developing baroclinic instability results in increasing imbalance; gravity waves are continuously initiated downstream of the maximum imbalance.

Gravity Wave Field in Weak Moist Run



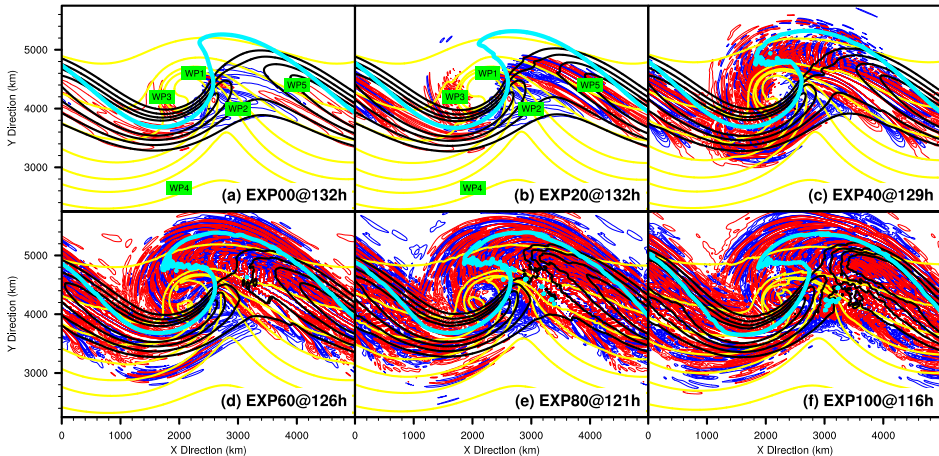
- In weak moist run, dry dynamic gravity wave modes continue to dominate, and moisture processes are believed to interact with, strengthen, and modify the dry gravity wave modes.

Gravity Wave Field in Full Moist Run



- Convective (moist) mode is soon fully coupled with other (dry) gravity wave modes and background flow as baroclinicity increases over time.

Simulations with Varying Initial Moisture

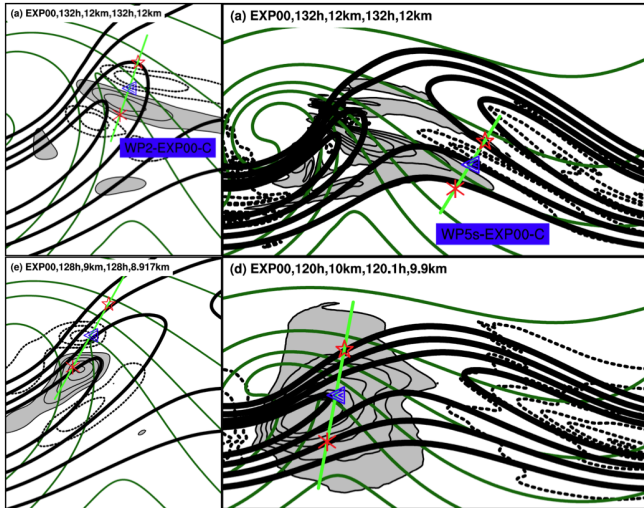


Simulated 1-km temperature (yellow lines), 8-km horizontal wind (black lines), 12-km horizontal divergence (blue/red lines)

Wei, J., and F. Zhang, 2014: Mesoscale Gravity Waves in Moist Baroclinic Jet-Front Systems. *J. Atmos. Sci.*, 71, 929–952.

Continuous Generation and Propagation

Same Source, Different Fate

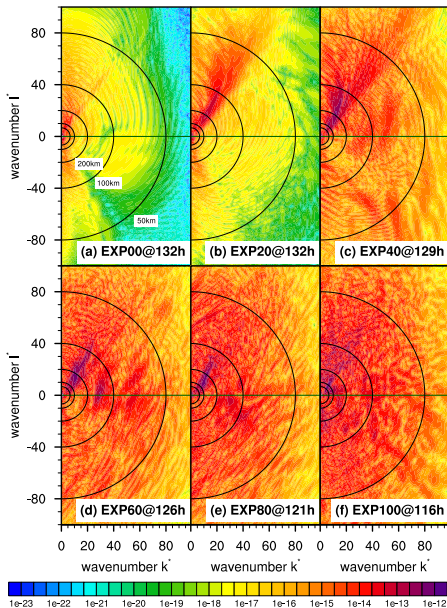


Wei, J., and F. Zhang, 2015: Tracking gravity waves in moist baroclinic jet-front systems. *J. Adv. Model. Earth Syst.*, 07, DOI: 10.1002/2014MS000395

Section 3

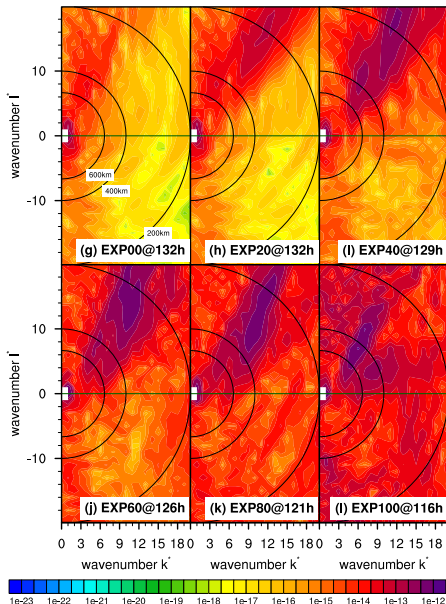
- 1 Introduction
- 2 Idealized Moist Jet/Front Waves
- 3 Spectral Characteristics**
- 4 Conclusion

2D FFT based on Divergence Field



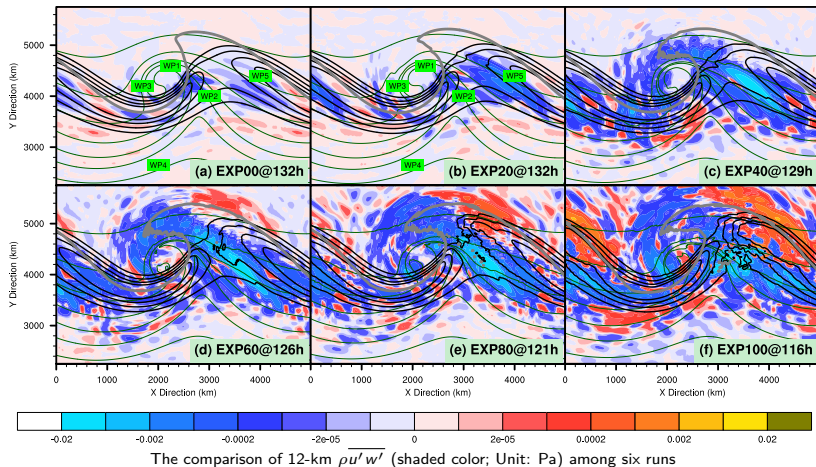
- For the short scales between 50 km and 200 km, the weak moist run of EXP20 has significant enhance of power along approximate 45 degree (relative to dry run).
- The distribution of power in strong convective cases (e.g., EXP80 and EXP100) appears to be more homogeneous along all angles (relative to EXP00 and EXP20)

2D FFT based on Divergence Field



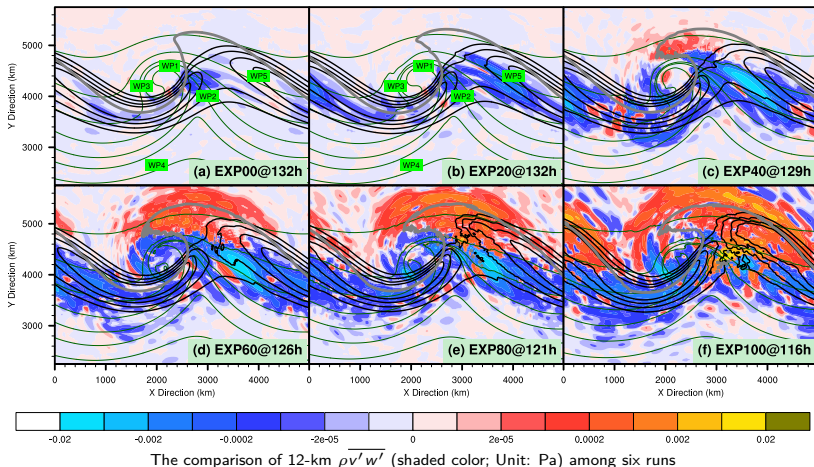
- EXP20 continues to have stronger power along approximate 45 degree (relative to EXP00).
- It is worth mentioning that the peak of power maxima along approximate 45 degree appears to migrate upscale.

Vertical Flux of Zonal Momentum (HRZ)



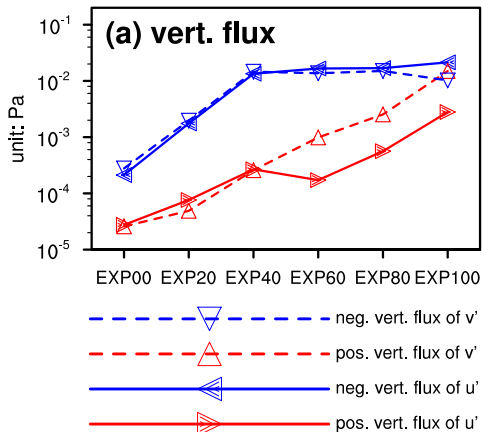
- The dominance of negative values in 12-km $\overline{\rho u' w'}$ (shaded color)
- Larger area of positive values for 12-km $\overline{\rho u' w'}$ in moist runs

Vertical Flux of Meridional Momentum (HRZ)

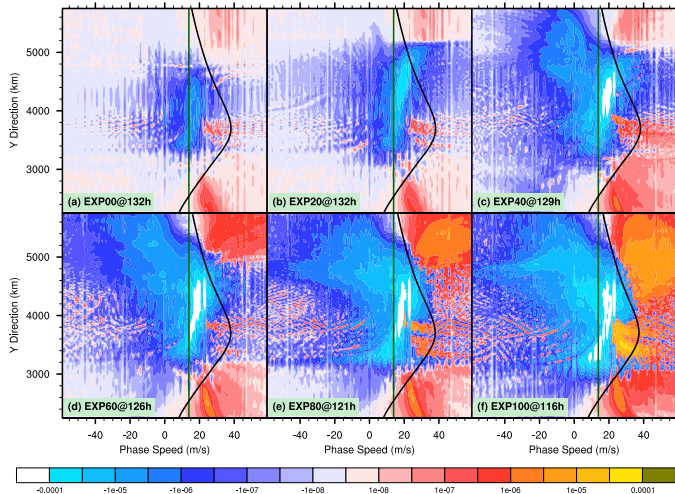


- In dry and weak moist runs, the dominance of negative values in 12-km $\overline{\rho v' w'}$
- In strong moist runs, both positive values and negative values are important.

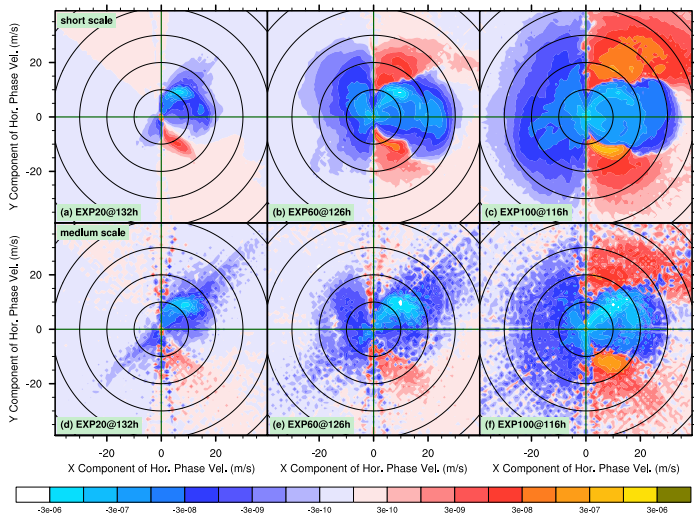
Max Momentum Flux



- The negative fluxes are generally much stronger than the positive fluxes, except for meridional momentum flux in EXP100.
- The result again emphasizes the role of moisture to obtain significant momentum fluxes, as highlighted in Plougonven et al (2015, J. Geophys. Res. Atmos.).

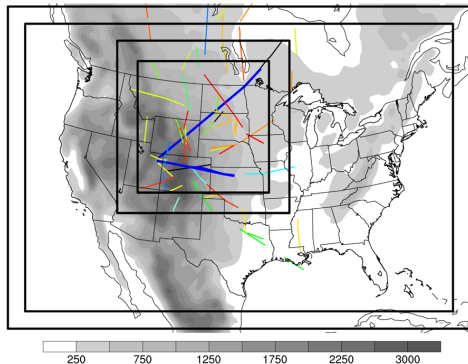
$\overline{\rho u' w'}$ versus c_{px} ($N_t \Delta t = 48hr$)


- Minimum of Negative Flux Locates Around BW Phase Speed ($\sim 13.9m/s$); Dipole Structure in EXP80 and EXP100

$\overline{\rho u' w'}$ versus 2D phase velocity


- The distribution for the short-scale component in the horizontal phase velocity space is more sensitive to the increasing initial moisture content.

Stratosphere-Troposphere Analyses of Regional Transport Experiment 2008 (START08)



Goals:

Targeting Major Transport Pathways in the Ex-UTLS

1. Extratropical UT/LS Survey (including cirrus clouds)
2. Stratospheric Intrusion (Tropopause Fold)
3. Tropospheric Intrusion
4. Convective Influence
5. Gravity Waves (RF 02)

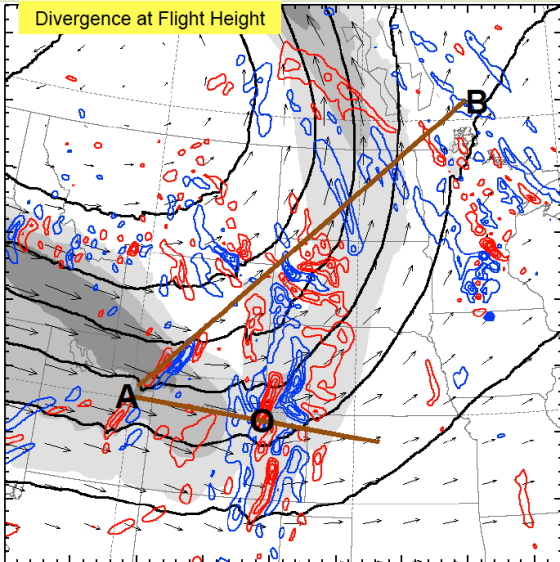
HIAPER Flight Tracks

(18 flights; Phase I: April 18-May 16; Phase II: June 16-27)

Zhang, F., J. Wei, M. Zhang, K. P. Bowman, L. L. Pan, E. Atlas, and S. C. Wofsy, 2015: Aircraft measurements of gravity waves in the upper troposphere and lower stratosphere during the START08 field experiment, *Atmos. Chem. Phys.*, 15, 7667-7684, doi:10.5194/acp-15-7667-2015.

Flight Track of RF-02 in START08

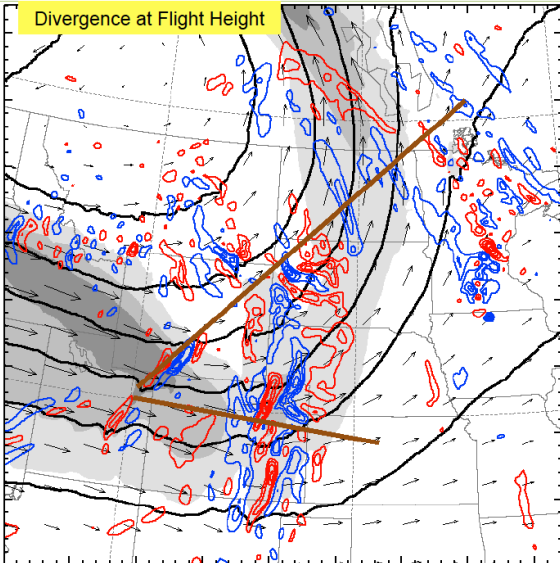
1.67-km WRF simulations at 2200 UTC 04/22/2008)



- Grey Shaded Area: 9-km Wind Speed (m/s)
- Blue/Red Contour: 12.5-km Divergence (pos/neg)
- Black Contour: 9-km Pressure (m)
- Vector: 9-km Wind Field (m/s)

Flight Track of RF-02 in START08

1.67-km WRF simulations at 2200 UTC 04/22/2008)



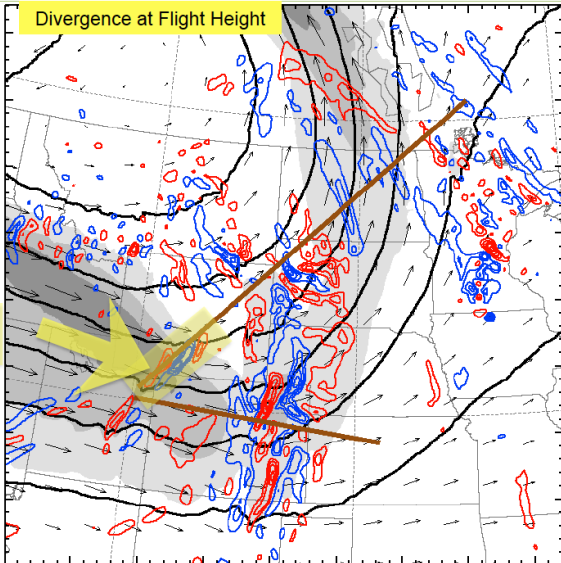
Possible Sources:

- Grey Shaded Area: 9-km Wind Speed (m/s)
- Blue/Red Contour: 12.5-km Divergence (pos/neg)
- Black Contour: 9-km Pressure (m)
- Vector: 9-km Wind Field (m/s)

Flight Track of RF-02 in START08

1.67-km WRF simulations at 2200 UTC 04/22/2008)

Possible Sources:
Northwesterly Jet

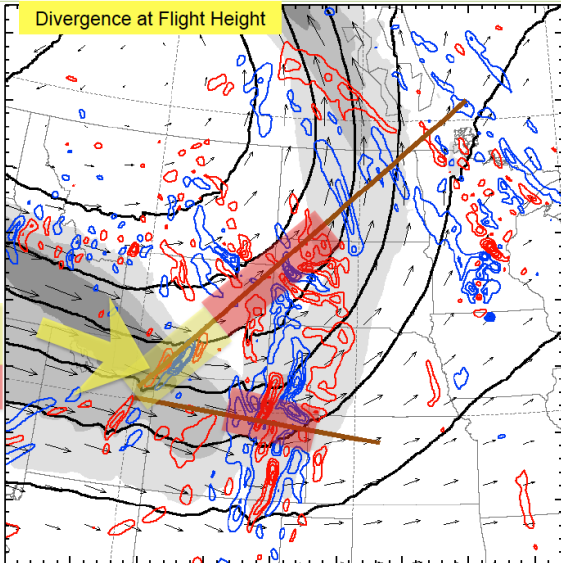


Direction of Mean Flow

- Grey Shaded Area: 9-km Wind Speed (m/s)
- Blue/Red Contour: 12.5-km Divergence (pos/neg)
- Black Contour: 9-km Pressure (m)
- Vector: 9-km Wind Field (m/s)

Flight Track of RF-02 in START08

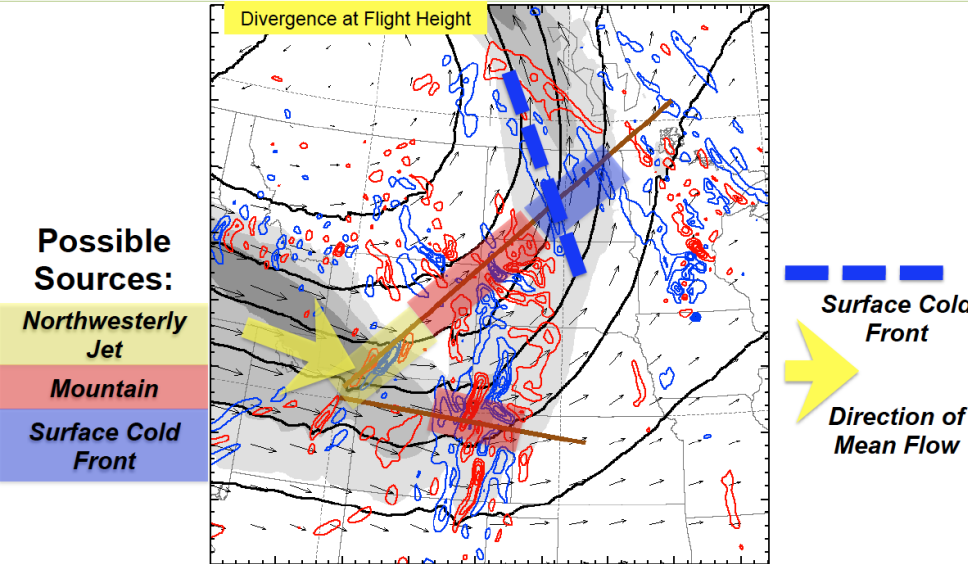
1.67-km WRF simulations at 2200 UTC 04/22/2008)



- Grey Shaded Area: 9-km Wind Speed (m/s)
- Blue/Red Contour: 12.5-km Divergence (pos/neg)
- Black Contour: 9-km Pressure (m)
- Vector: 9-km Wind Field (m/s)

Flight Track of RF-02 in START08

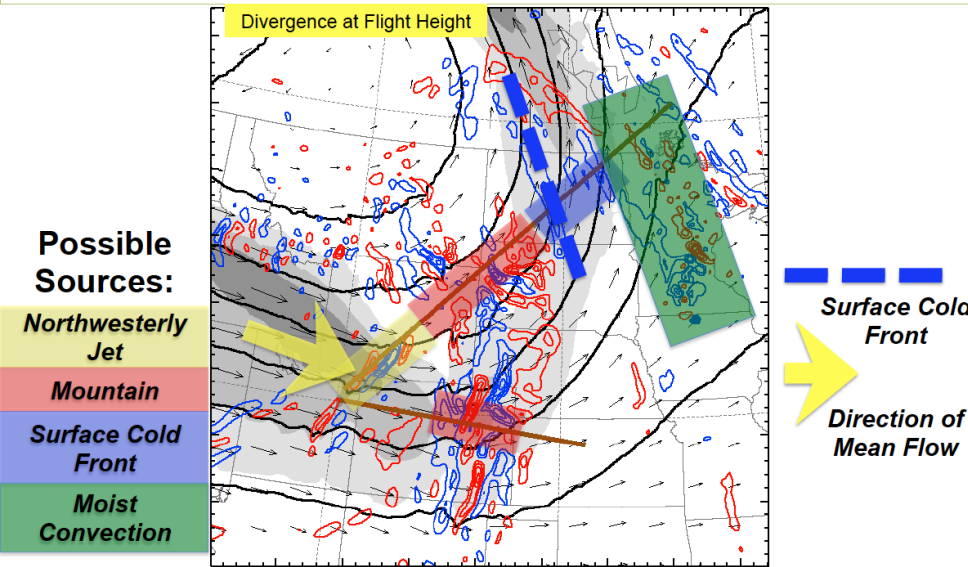
1.67-km WRF simulations at 2200 UTC 04/22/2008)



- Grey Shaded Area: 9-km Wind Speed (m/s)
- Blue/Red Contour: 12.5-km Divergence (pos/neg)
- Black Contour: 9-km Pressure (m)
- Vector: 9-km Wind Field (m/s)

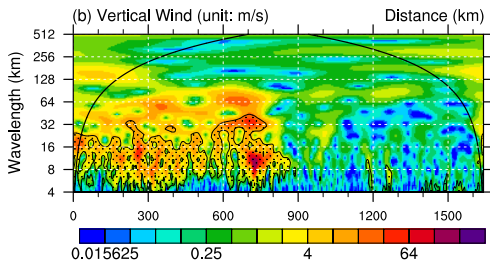
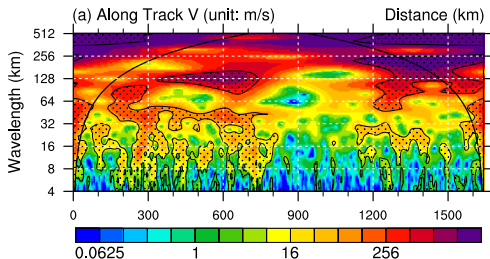
Flight Track of RF-02 in START08

1.67-km WRF simulations at 2200 UTC 04/22/2008)



- Grey Shaded Area: 9-km Wind Speed (m/s)
- Blue/Red Contour: 12.5-km Divergence (pos/neg)
- Black Contour: 9-km Pressure (m)
- Vector: 9-km Wind Field (m/s)

Zhang et al. (2015, ACP) on START08



- The aircraft sampled a wide range of background conditions with clear evidence of vertically propagating mesoscale gravity waves of along-track wavelength between 100 and 120 km.
- At least part of the nearly periodic high-frequency signals might be a result of intrinsic observational errors in the aircraft measurements.

Please also see the below paper on the potential aircraft measurement error:

Hansman, R. J., and J. Sturdy, 1989: Dynamic Response of Aircraft-Autopilot Systems to Atmospheric Disturbances, *Journal of Aircraft*, 26, No. 2, 124-130.

Section 4

- 1 Introduction
- 2 Idealized Moist Jet/Front Waves
- 3 Spectral Characteristics
- 4 Conclusion

Conclusion

- In weak moist run, dry dynamic gravity wave modes continue to dominate, and moisture processes are believed to interact with, strengthen, and modify the dry gravity wave modes. In full moist run, moisture processes are soon fully coupled with other gravity wave modes and background flow as baroclinicity increases over time.

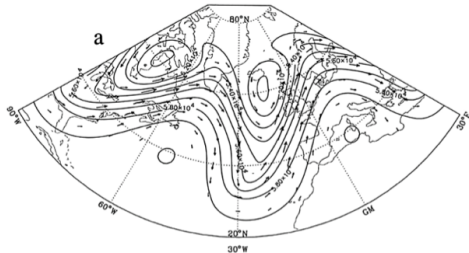
Wei, J., and F. Zhang, 2014: Mesoscale Gravity Waves in Moist Baroclinic Jet-Front Systems. *J. Atmos. Sci.*, 71, 929–952.

- It emphasizes the role of moisture to obtain significant momentum fluxes.
- It is confirmed that the dry gravity wave source generates a relatively narrow and less symmetrical power spectrum centered around lower phase speeds and horizontal wavenumbers, whereas the moist gravity wave source generates a broader and more symmetrical power spectrum, with a broader range of phase speeds and horizontal wavenumbers.

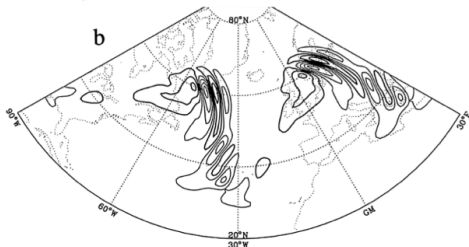
Wei, J., F. Zhang, and J. H. Richter, 2016: An Analysis of Gravity Wave Spectral Characteristics in Moist Baroclinic Jet-Front Systems. *J. Atmos. Sci.*. Accepted.

Dry Idealized Simulations

Geopotential Height and Wind at 503 hPa



Divergence of the Horizontal Wind at 130 hPa



O'Sullivan and Dunkerton (1995, JAS)

- Based on a 3D hydrostatic primitive equation model with coarse horizontal resolution (50-100 km)
- Gravity waves generated in the upper-tropospheric jet exit region
- Wave characteristics
 - $\lambda_H \sim 600-1000\text{km}$ (sub-synoptic scale)
 - $\Omega \sim 1-2f$ (low frequency)

Wave Capturing

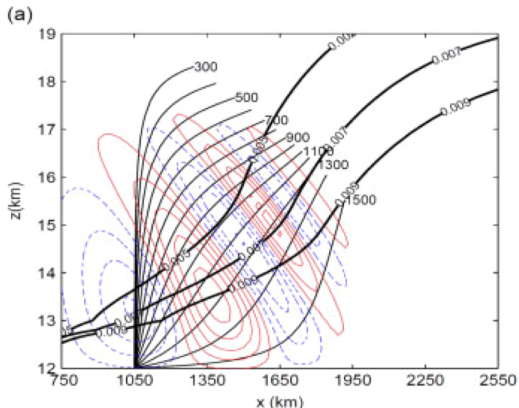
**Effect of
background flow
deformation: result
with ray tracing
(Lin and Zhang 2008 JAS;
Marks/Eckermann 1995 JAS)**

**releasing rays at jet
exit with initial
 $L_x=300-1500\text{km}$**

wave capturing?!

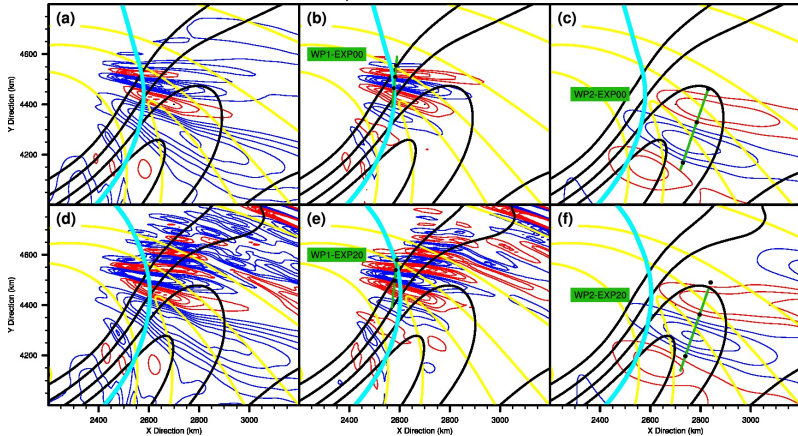
**mid thick line:
 $k/m \sim U_x/U_z$
 $\sim f/N \sim 0.007 \text{ s}^{-1}$**

(Wang, Zhang, Epifanio 2010 QJ)



Part II: Moist Simulations

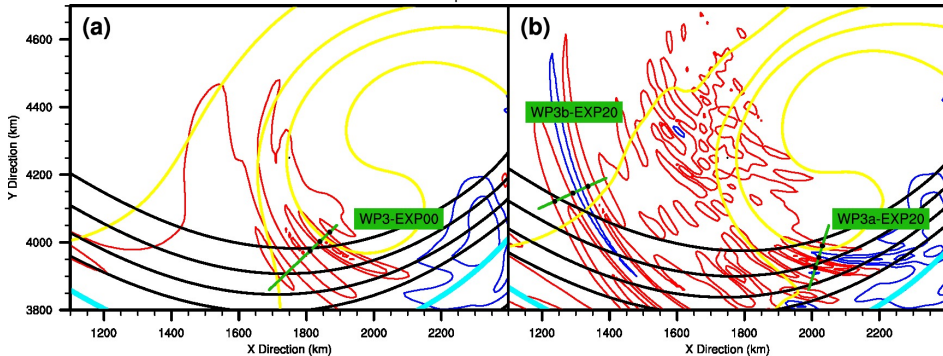
Examples of WP1 and WP2



	λ_H	λ_z	Ω		λ_H	λ_z	Ω
WP1-EXP00	90km	1.7km	3.9f	WP2-EXP00	310km	2.8km	2.2f
WP1-EXP20	83km	1.7km	4.2f	WP2-EXP20	310km	2.8km	2.2f

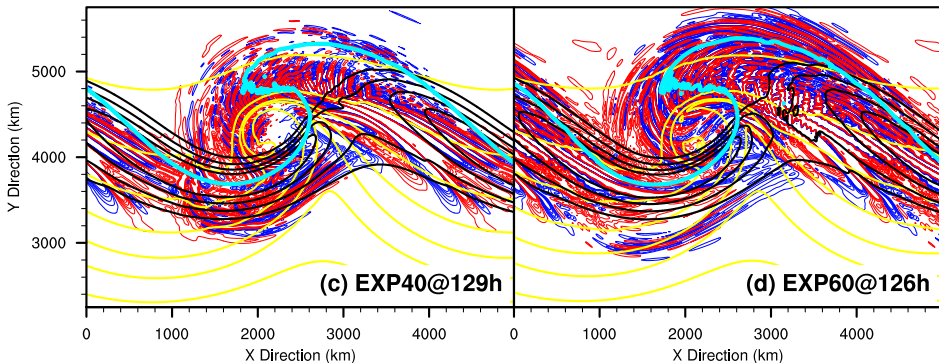
Part II: Moist Simulations

Examples of WP3



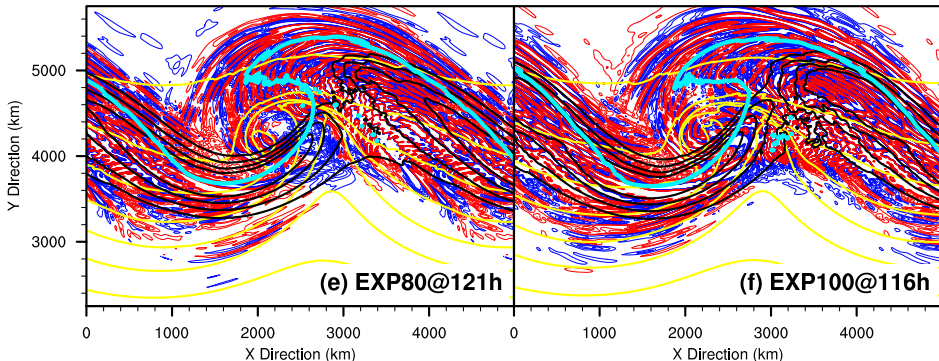
	λ_H	λ_z	Ω
WP3-EXP00	80km	6.2km	14.6f
WP3a-EXP20	68km	4.9km	13.5f
WP3b-EXP20	108km	6.1km	11.0f

Moderate Convective Instability



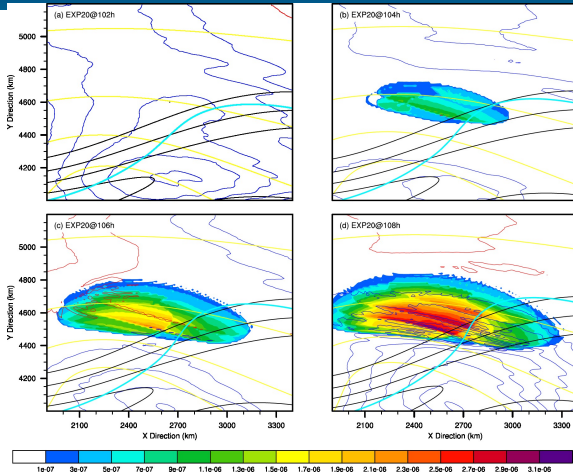
- EXP40: Both Shorter-Scale Waves and Intermediate-Scale Waves Are Essential.
- EXP60: More Variances of Shorter-Scale Gravity Waves In the Jet Exit Region.

Strong Convective Instability



- EXP80: Shorter-Scale Wave Signatures Filling the Jet; Imprint of Intermediate-Scale Wave Signatures South of the Upper-Level Northwesterly Jet
- EXP100: Particularly Hard to Determine the Dominant Orientation of Wave Front South of the Upper-Level Northwesterly Jet

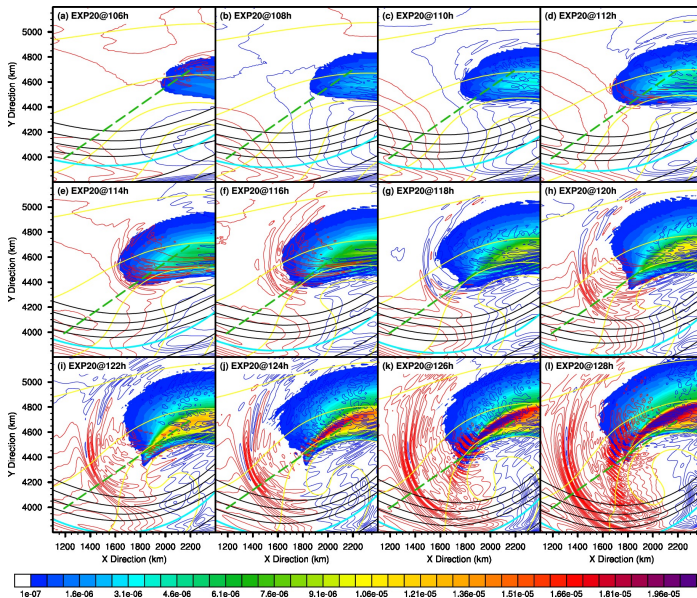
Local Effect



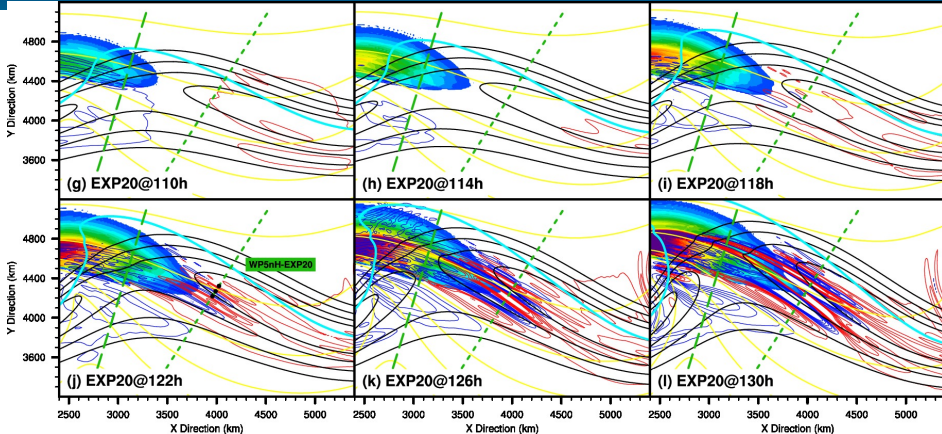
The shaded color denote the positive-only latent heating rate (K/s).

- Local convection associated with latent heating release may be the potential source mechanism for the generation of WP6.

Upstream Effect

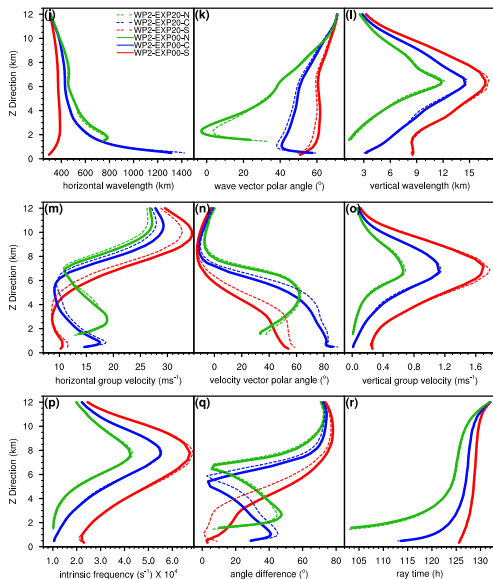


Downstream Effect



- Differences in gravity waves may travel from upstream localized convection toward downstream jet entrance region.

Medium-Scale Waves in Jet-Exit Region



- The three-stage conceptual model: (1) Slow vertical propagation way above the tropopause (the first stage); (2) Fast vertical propagation around the tropopause (the second stage); (3) Slow vertical propagation way below tropopause (the third stage).
- The vertical profiles of propagating wave characteristics of WP2 between dry run (three solid lines) and weak moist run (three dash lines) are almost identical.

Vertical profiles of WP2 in dry run and weak moist run

Ray Tracing Equation

The Gravity Wave Regional or Global Tracer (GROGRAT) model Marks and Eckermann (1995); Eckermann and Marks (1996; 1997)

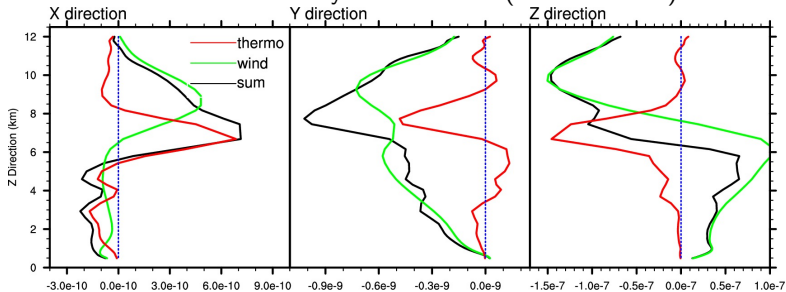
- ◆ The first three terms in the RHS are considered as **wind (shear) terms**.
- ◆ The fourth and fifth terms in the RHS are considered as **thermodynamics (shear) terms**.

	wind (shear) terms	thermodynamics (shear) terms	
$\frac{d_g k}{dt}$	$-ku_x - lv_x - mw_x$	$-\frac{N_x^2(k^2 + l^2)}{2\Omega\Delta} + \frac{\alpha_x^2(\Omega^2 - f^2)}{2\Omega\Delta}$	
$\frac{d_g l}{dt}$	$-ku_y - lv_y - mw_y$	$-\frac{N_y^2(k^2 + l^2)}{2\Omega\Delta} + \frac{\alpha_y^2(\Omega^2 - f^2)}{2\Omega\Delta}$	$\frac{ff_y(m^2 + \alpha^2)}{\Omega\Delta}$
$\frac{d_g m}{dt}$	$-ku_z - lv_z - mw_z$	$-\frac{N_z^2(k^2 + l^2)}{2\Omega\Delta} + \frac{\alpha_z^2(\Omega^2 - f^2)}{2\Omega\Delta}$	

Budget Analysis in Wavenumber Refraction

Budget Analysis of WP2 in Dry Run

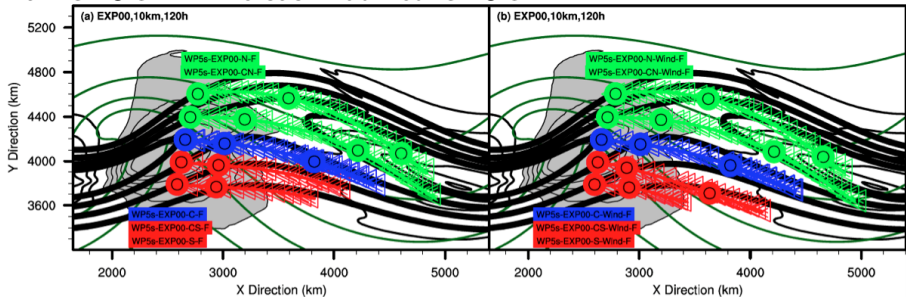
Wind Terms versus Thermodynamics Terms (unit: $m^{-1}s^{-1}$)



- For most part of the backward ray tracing, the wind terms are dominant.
- However, the thermodynamics terms can potentially enhance or even largely cancel the effect of the wind terms around the tropopause or surface frontal systems, in which there is dramatic change in static stability.
- Generally, for an upward-propagating wave packet crossing the tropopause, the thermodynamics effect tends to shorten the vertical wavelength.

Southern Part of the Fifth Wave Packet

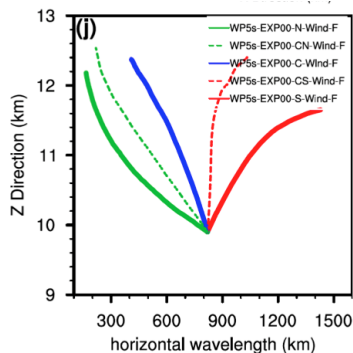
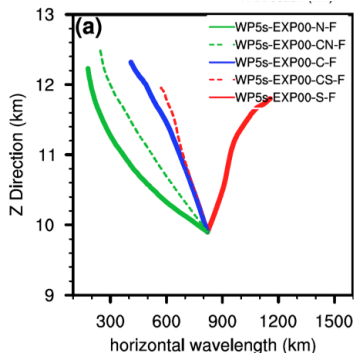
Forward Ray Tracing of WP5s-EXP00: Full GROGRAT Versus Modified GROGRAT



- There may be sensitivity to the inclusion/exclusion of the thermodynamics effect for certain baroclinic jet exit wave packets in their ray trajectories (e.g., the tendency of southward propagation) and the propagating wave characteristics (e.g., the shrinkage in wavelengths).

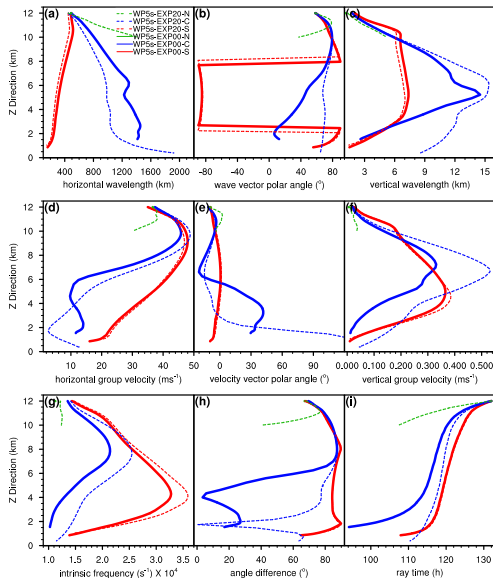
Southern Part of the Fifth Wave Packet

Forward Ray Tracing of WP5s-EXP00:
 Full GROGRAT Versus Modified GROGRAT



- There may be sensitivity to the inclusion/exclusion of the thermodynamics effect for certain baroclinic jet exit wave packets in their ray trajectories (e.g., the tendency of southward propagation) and the propagating wave characteristics (e.g., the shrinkage in wavelengths).

Southern Part of the Fifth Wave Packet

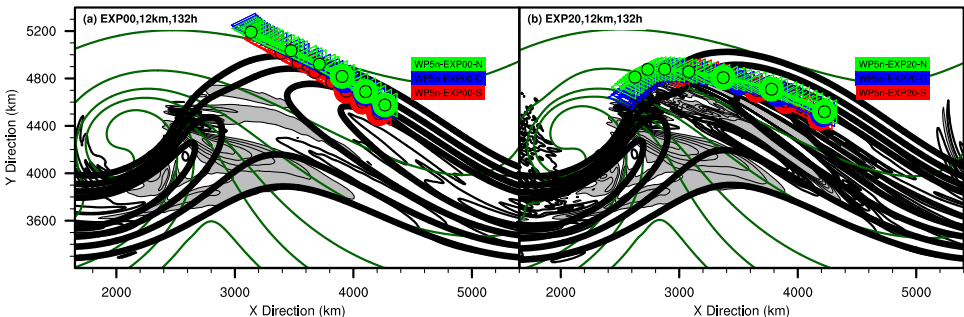


Vertical profiles of WP5s in dry run and weak moist run

- The propagating wave characteristics and the life cycles of the three selected rays for WP5s are rather different from each other.
- Convection may partially impact the amplitude and wave characteristics of WP5s-EXP20, since the upper-level jet exit region is also very close to the low-level convection in the horizontal views.

The Sensitivity of Trajectories to Moisture

The Trajectories of WP5n in Dry Run versus Those in Weak Moist Run

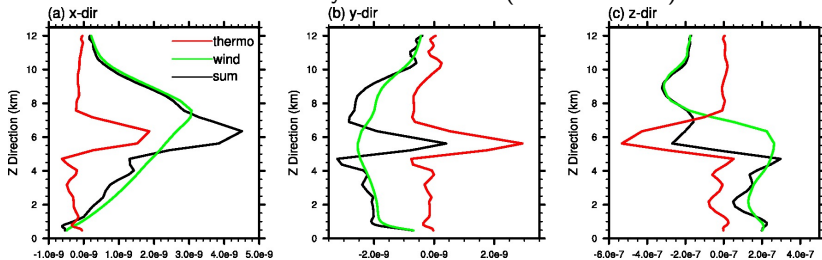


- The horizontal views of the tracks of WP5n between dry run and weak moist run are somewhat distinct from one another.
- The WP5n in weak moist run can be traced back to the divergence disturbance associated with the initial convection below the tropopause.

Budget Analysis in Wavenumber Refraction

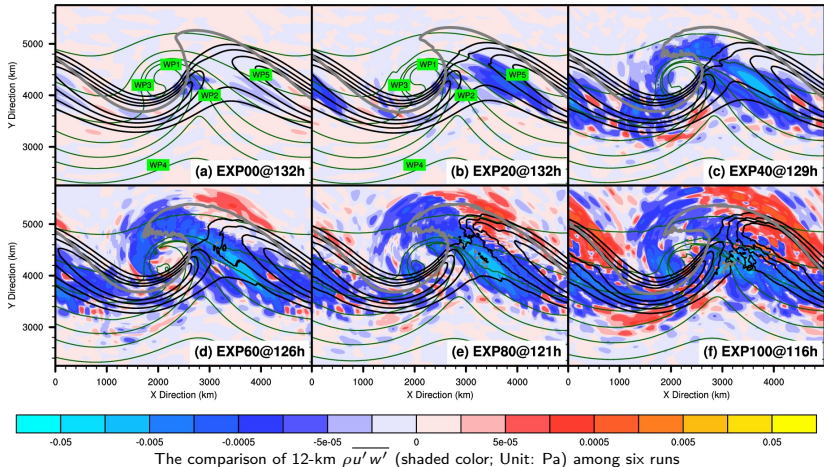
Budget Analysis of WP1 in Dry Run

Wind Terms versus Thermodynamics Terms (unit: $m^{-1}s^{-1}$)



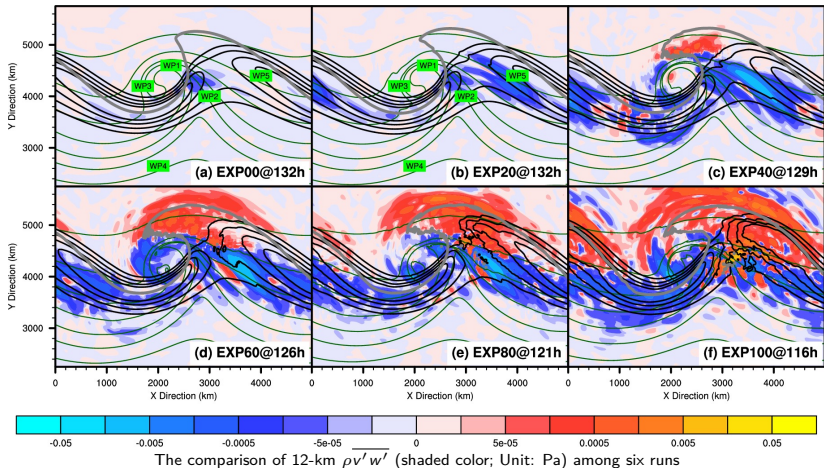
- For most part of the backward ray tracing, the wind terms are dominant.
- However, the thermodynamics terms can potentially enhance or even largely cancel the effect of the wind terms around the tropopause or surface frontal systems, in which there is dramatic change in static stability.
- Generally, for an upward-propagating wave packet crossing the tropopause, the thermodynamics effect tends to shorten the vertical wavelength.

Vertical Flux of Zonal Momentum (HRZ)



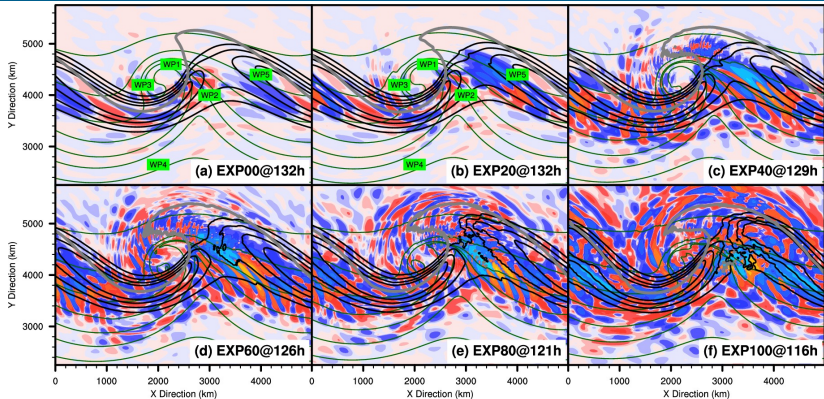
- The dominance of negative values in 12-km $\overline{\rho u' w'}$ (shaded color)
- Larger area of positive values for 12-km $\overline{\rho u' w'}$ in moist runs

Vertical Flux of Meridional Momentum (HRZ)



- In dry and weak moist runs, the dominance of negative values in 12-km $\overline{\rho v' w'}$
- In strong moist runs, both positive values and negative values are important.

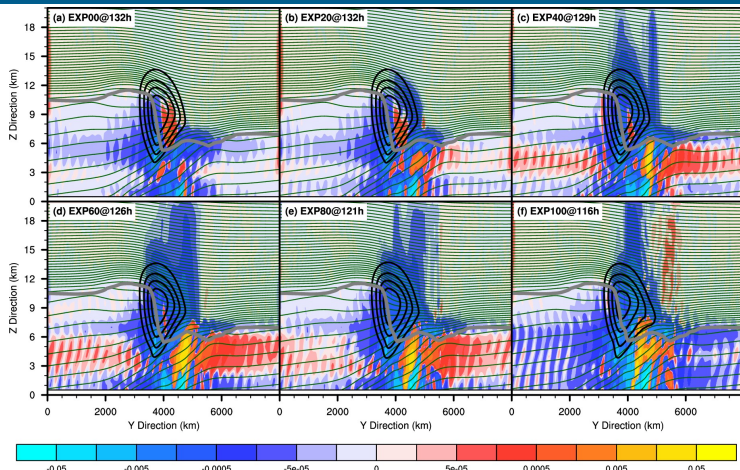
Wave-Induced Forcing of Zonal Flow (HRZ)



The comparison of 12-km $-\frac{1}{\rho} \frac{\partial \overline{\rho u' w'}}{\partial z}$ (shaded color; Unit: $ms^{-1}s^{-1}$) among six runs

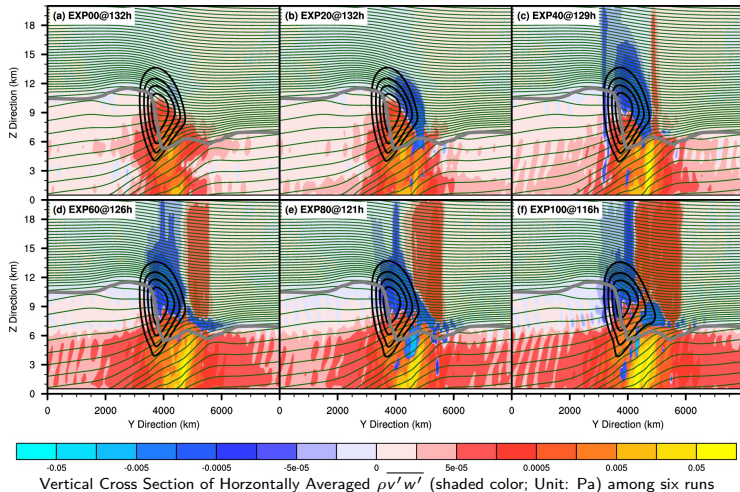
- Wave-like structure in 12-km horizontal distributions of $-\frac{1}{\rho} \frac{\partial \overline{\rho u' w'}}{\partial z}$;
- The 12-km $-\frac{1}{\rho} \frac{\partial \overline{\rho u' w'}}{\partial z}$ looks different from the 12-km $\overline{\rho u' w'}$

Vertical Flux of Zonal Momentum (CRS)



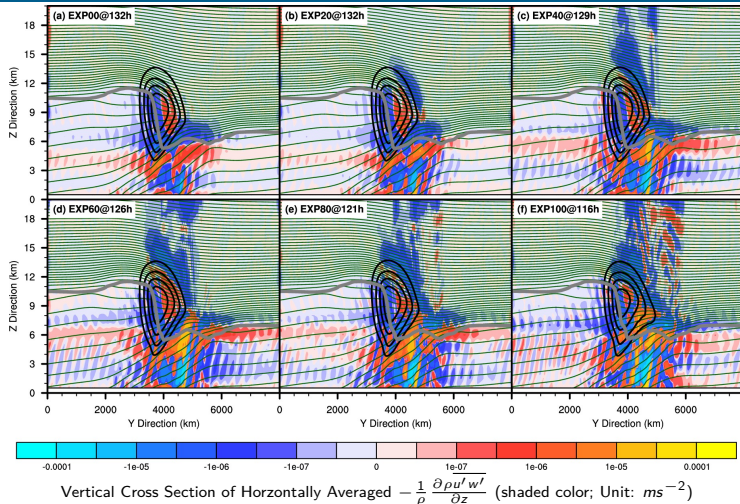
- General consistent pattern of $\overline{\rho u' w'}$ among all the experiments
- More chances of high-level waves with negative $\overline{\rho u' w'}$ in moist runs

Vertical Flux of Meridional Momentum (CRS)



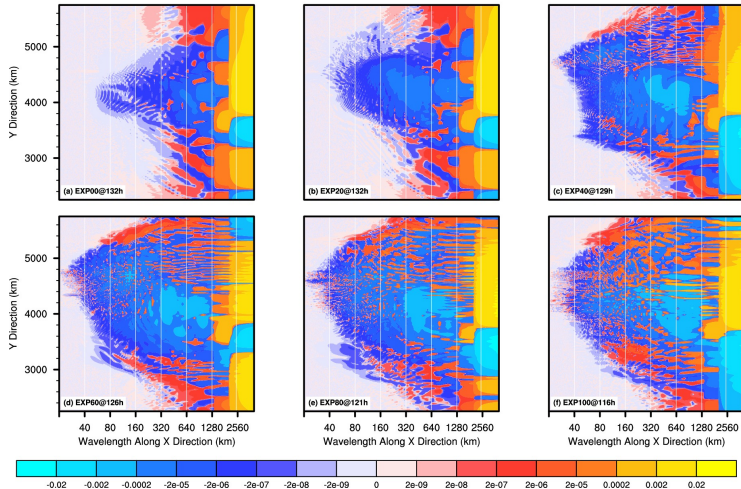
- In strong moist runs, both positive values and negative values of $\overline{\rho v' w'}$ are important.

Wave-Induced Forcing of Zonal Flow (CRS)



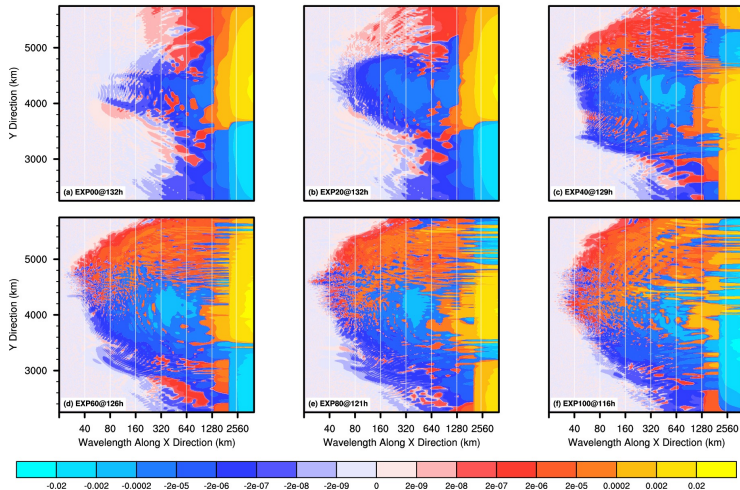
- General consistent pattern of $-\frac{1}{\rho} \frac{\partial \overline{\rho u' w'}}{\partial z}$ among all the experiments; Similarity between wave-induced forcing and momentum flux in CRS

$\overline{u'w'}$ versus k

 12-km cospectrum of u' & w' (color shading) at each latitude (smth=0; taper=0%)


- Negative Flux Valley Appears to Be Saturated in EXP40
- Sensitivity to Moisture for the Flux Below the Scale of 80 km

$\overline{v'w'}$ versus k

 12-km cospectrum of v' & w' (color shading) at each latitude (smth=0; taper=0%)


- South of $y=4600$ km, $\overline{v'w'}$ is dominated by negative values.
- An arguable dominance of positive values north of $y=4000$ km

Ray Tracing Equation

The Gravity Wave Regional or Global Tracer (GROGRAT) model Marks and Eckermann (1995); Eckermann and Marks (1996; 1997)

$$\frac{d_g x}{dt} = u + \frac{k(N^2 - \Omega^2)}{\Omega\Delta} = C_{gx}$$

$$\frac{d_g y}{dt} = v + \frac{l(N^2 - \Omega^2)}{\Omega\Delta} = C_{gy}$$

$$\frac{d_g z}{dt} = w - \frac{m(\Omega^2 - f^2)}{\Omega\Delta} = C_{gz}$$

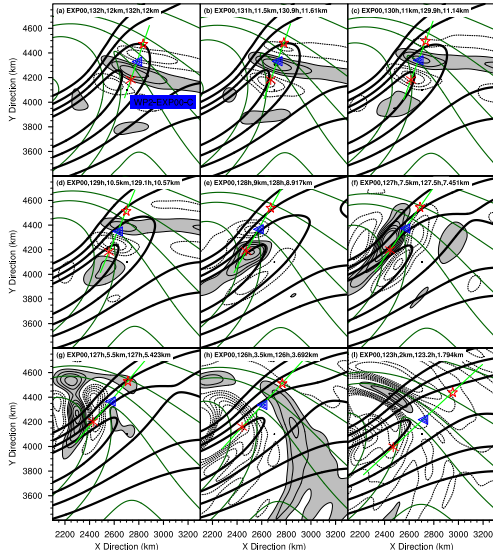
The ray tracing equations describe the propagating trajectory and wavenumber vector refraction.

$$\frac{d_g k}{dt} = -ku_x - lv_x - mw_x - \frac{N_x^2(k^2 + l^2)}{2\Omega\Delta} + \frac{\alpha_x^2(\Omega^2 - f^2)}{2\Omega\Delta}$$

$$\frac{d_g l}{dt} = -ku_y - lv_y - mw_y - \frac{N_y^2(k^2 + l^2)}{2\Omega\Delta} + \frac{\alpha_y^2(\Omega^2 - f^2)}{2\Omega\Delta} - \frac{ff_y(m^2 + \alpha^2)}{\Omega\Delta}$$

$$\frac{d_g m}{dt} = -ku_z - lv_z - mw_z - \frac{N_z^2(k^2 + l^2)}{2\Omega\Delta} + \frac{\alpha_z^2(\Omega^2 - f^2)}{2\Omega\Delta}$$

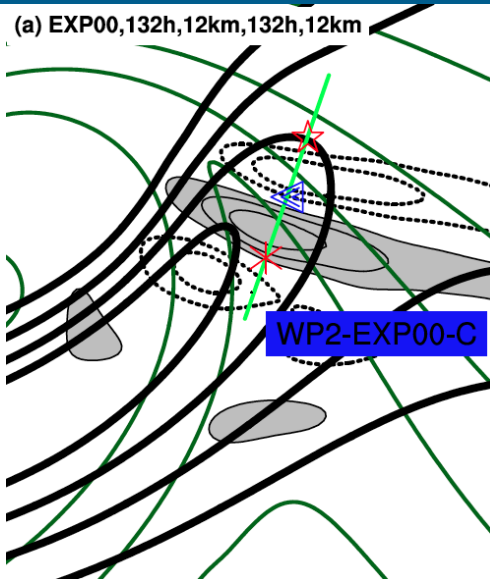
Medium-Scale Waves in Jet-Exit Region



Horizontal views of WP2-EXP00-C in EXP00 at each selective time during its backward and downward integrations.

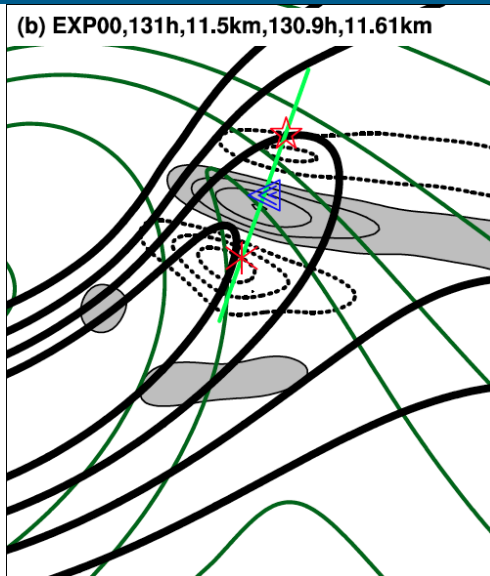
- The position, the horizontal wavelength, and the horizontal wave vector polar angle of WP2-EXP00-C from GROGRAT match the WRF-simulated horizontal divergence fields quite well from 12 km to 10.5 km (from 132 h to ~ 129 h).
- Noticeable discrepancy between GROGRAT and WRF at ~ 9.0 km, which becomes more severe from ~ 7.5 to ~ 5.5 km.
- The potential source of WP2-EXP00 may be the upper-tropospheric jet-front system.

Medium-Scale Waves in Jet-Exit Region



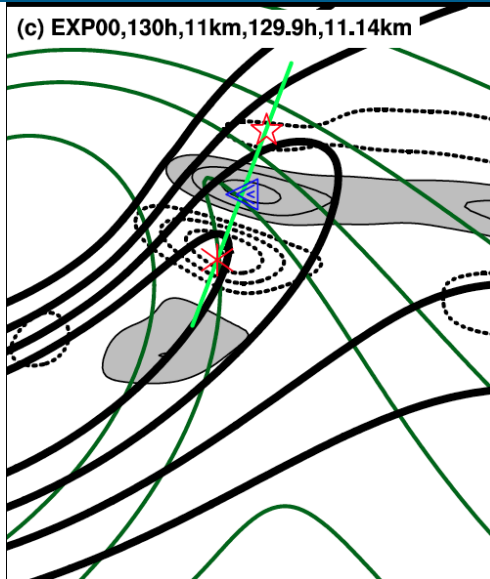
Horizontal views of WP2-EXP00-C in EXP00 at each selective time during its backward and downward integrations.

Medium-Scale Waves in Jet-Exit Region



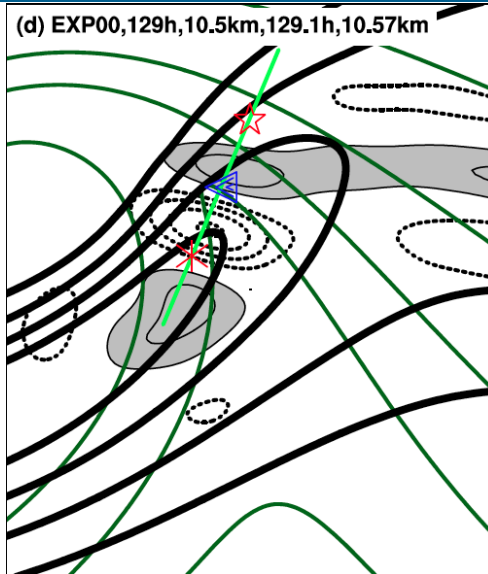
Horizontal views of WP2-EXP00-C in EXP00 at each selective time during its backward and downward integrations.

Medium-Scale Waves in Jet-Exit Region



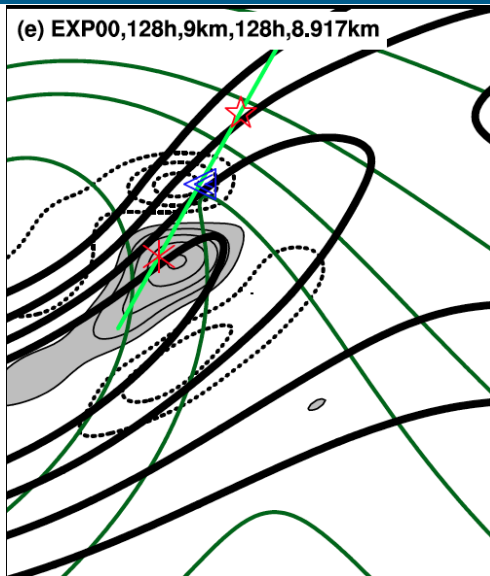
Horizontal views of WP2-EXP00-C in EXP00 at each selective time during its backward and downward integrations.

Medium-Scale Waves in Jet-Exit Region



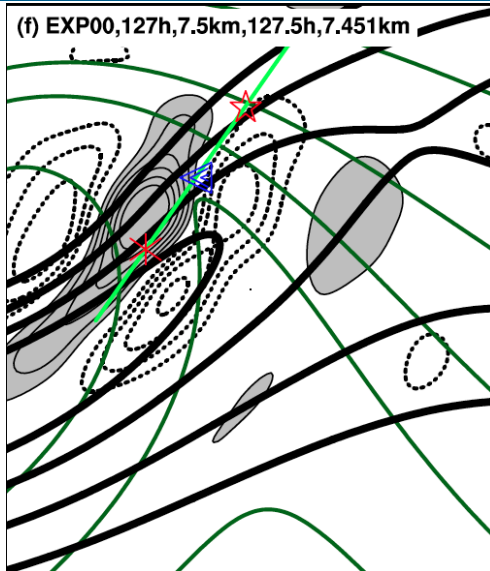
Horizontal views of WP2-EXP00-C in EXP00 at each selective time during its backward and downward integrations.

Medium-Scale Waves in Jet-Exit Region



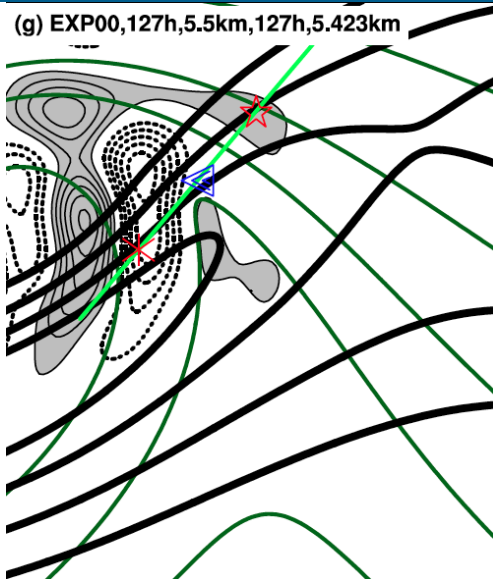
Horizontal views of WP2-EXP00-C in EXP00 at each selective time during its backward and downward integrations.

Medium-Scale Waves in Jet-Exit Region



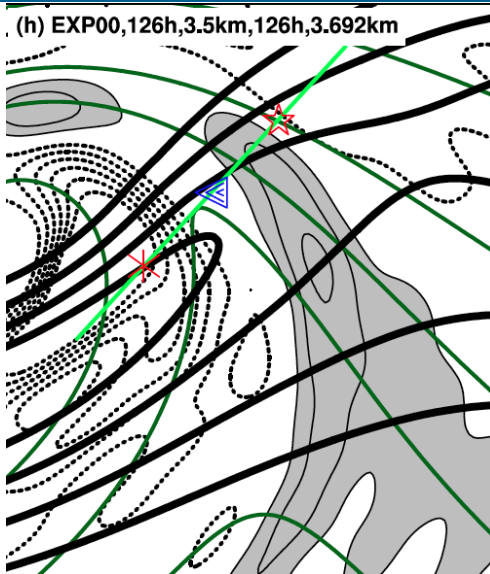
Horizontal views of WP2-EXP00-C in EXP00 at each selective time during its backward and downward integrations.

Medium-Scale Waves in Jet-Exit Region



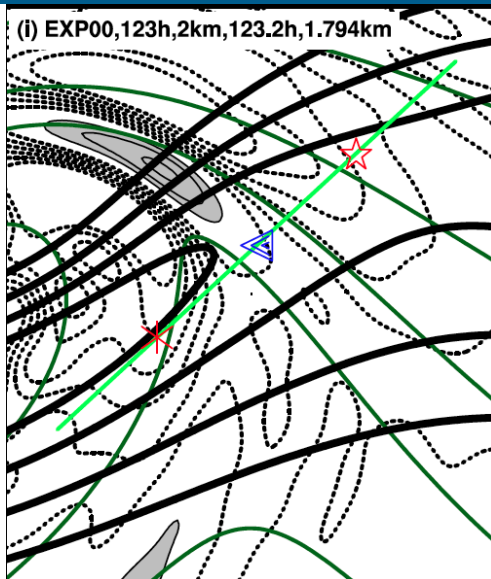
Horizontal views of WP2-EXP00-C in EXP00 at each selective time during its backward and downward integrations.

Medium-Scale Waves in Jet-Exit Region



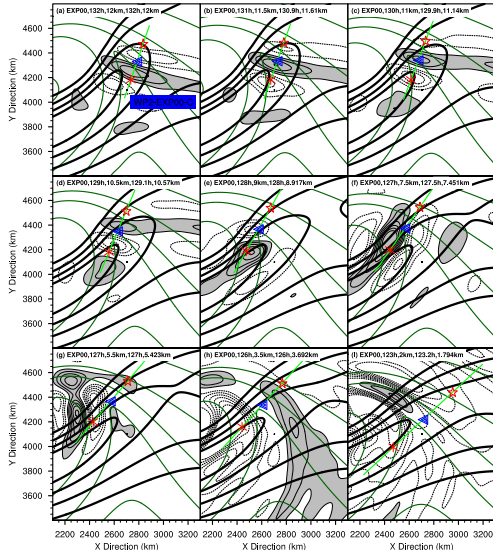
Horizontal views of WP2-EXP00-C in EXP00 at each selective time during its backward and downward integrations.

Medium-Scale Waves in Jet-Exit Region



Horizontal views of WP2-EXP00-C in EXP00 at each selective time during its backward and downward integrations.

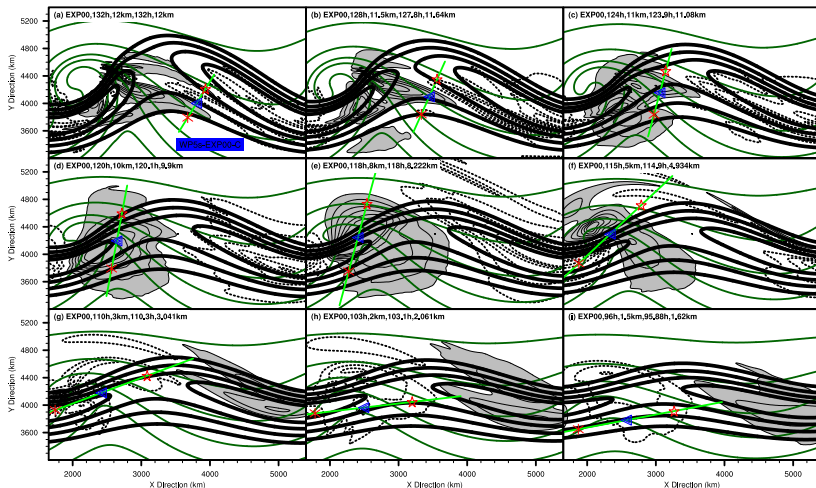
Medium-Scale Waves in Jet-Exit Region



Horizontal views of WP2-EXP00-C in EXP00 at each selective time during its backward and downward integrations.

- The position, the horizontal wavelength, and the horizontal wave vector polar angle of WP2-EXP00-C from GROGRAT match the WRF-simulated horizontal divergence fields quite well from 12 km to 10.5 km (from 132 h to ~ 129 h).
- Noticeable discrepancy between GROGRAT and WRF at ~ 9.0 km, which becomes more severe from ~ 7.5 to ~ 5.5 km.
- The potential source of WP2-EXP00 may be the upper-tropospheric jet-front system.

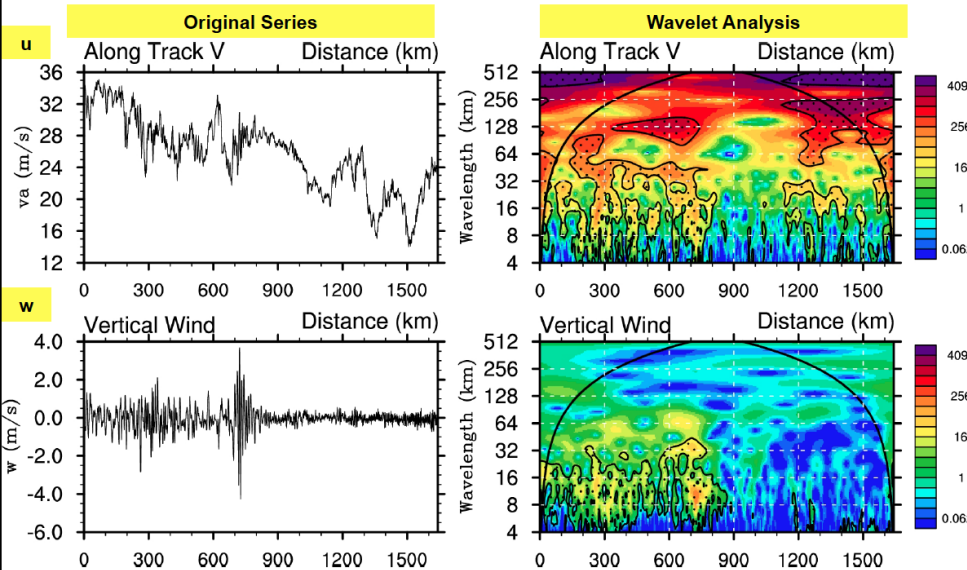
Southern Part of the Fifth Wave Packet



Horizontal views of WP5s-EXP00-C in EXP00 at each selective time during its backward and forward integrations.

- The potential source of WP5s-EXP00 may be upper-tropospheric jet/front.

Wavelet Analysis of Aircraft Measurements: Southbound Leg Along Jet



Wavelet Analysis for Southbound Leg Along Jet. Shaded Area Represent Significant Level Over 95%

- Significant Localized Variations of Wave Signal
- Mesoscale Gravity Wave in Along-Track velocity

- Possible Wave-Wave Interaction
- Physical Reliability of 10-km Wave in W